THE DECREPITATION OF SOLIDIFIED HIGH TITANIA SLAGS

By

D Bessinger, JMA Geldenhuis, PC Pistorius, A Mulaba and G Hearne

D Bessinger, Principal Engineer, Iscor R&D, ISCOR, P.O. Box 450 Pretoria 0001, Telephone no. (012) 307 7792, Fax no. (012) 307 7407, E-mail deonb@iscorltd.co.za

J.M.A. Geldenhuis, Professor, Department of Materials Science and Metallurgical Engineering, University of Pretoria, Pretoria 0001, Telephone no. (012) 420 3191, E-mail kgeldenh@postino.up.ac.za

P.C. Pistorius, Professor, Department of Materials Science and Metallurgical Engineering, University of Pretoria, Pretoria 0001, Telephone no. (012) 420 3922, E-mail pistori@postino.up.ac.za

A Mulaba, Lecturer, Metallurgy Department, Faculty of Mining and Metallurgy, Technikon Witwatersrand, P.O. Box 17011 Doornfontein, Johannesburg, Telephone no. (011) 406 2335/51, E-mail MULABA@physnet.phys.wits.ac.za

G Hearne, Senior Lecturer, Department of Physics, University of the Witwatersrand, Private Bag X3, Wits 2050, Johannesburg, Telephone no. (011) 716 2074/2526, E-mail Hearne@physnet.phys.wits.ac.za

SYNOPSIS

The decrepitation of high titania slags poses a problem for slag producers in that a larger amount of fine slag (-106 µm) is produced. This results in a lower income per ton of slag. In this study the decrepitation of high titania slags under oxidizing conditions was studied in an attempt to identify the causes of the decrepitation.

Decrepitation of titania slags were observed after heating at 400 °C. This phenomenon was however not observed after heating the slags at higher temperatures. From the available literature and experimental information it is postulated that the decrepitation occurs due to changes in the crystal chemistry of the M_3O_5 phase in the slag. The Mössbauer spectroscopy technique has proved very useful in elucidating the crystal-chemical details of the iron-bearing phases and their potential impact on the mechanisms responsible for decrepitation. It is recommended that further work be carried out using this technique to fully explain the transformations that occur.

1 INTRODUCTION

1.1 Background

High titania slag is produced during the smelting of ilmenite in a furnace with a suitable carbonaceous reductant. In this process a large fraction of the iron content of the ilmenite is reduced to metallic iron. The remainder of the material essentially collects in a high titania slag. The iron and slag are tapped through separate tapholes, with the titania slag being the higher value product. The slag is typically tapped into moulds that would yield 20 ton slag blocks. After the slag cooling process, which can last approximately seven to ten days, the slag is crushed and milled to produce a fine and coarse product. These products are used in the downstream processing for the production of titanium dioxide pigment. The fine slag product (-106 µm) is used by the sulphate processing route, while the coarser product (-850+106 µm) is used by the chloride processing route. The coarse slag product has a higher value than the fine slag product.

During the slag cooling process severe decrepitation of the slag may occur. Decrepitation of the slag is detrimental because an excess of fine material (-106 µm) is produced. It is important to produce a minimum amount of fine slag in order to maximize the income that can be derived from titania slag. This investigation was undertaken to study the decrepitation of high titania slag to gain an understanding of the factors influencing decrepitation. In this study decrepitation is defined as the disintegration or crumbling of a material into component parts or fragments.

1.2 Literature survey on the decrepitation of slags

Decrepitation of slag is a fairly well known phenomenon, especially for steelmaking slags. Decrepitation of slag occurs due to phase and chemical changes in the slag, and the resultant volume changes associated with these phase changes. Examples of the decrepitation of slags are the following:

- The decrepitation of steelmaking slags due to an increase in volume of the free lime in the slag during hydration[1,2]. This is particularly a problem in the cement industry.
- A second well-known example is that of the disintegration on cooling of slag containing dicalcium silicate (Ca_2SiO_4)[3]. This is due to a transition from the β (monoclinic structure) to γ (rhombohedral structure) polymorph. This transition is accompanied by an expansion in volume of approximately 10 per cent.

Very little has been published in the open literature on the oxidation and decrepitation behaviour of high titania slags. Vasyutinskiy and Movsesov[4] studied the oxidation and grinding of a high titania slag containing 90.1 per cent TiO_2 and 3.47 per cent FeO. It was concluded that in order to obtain the maximum reduction in strength of the slag, oxidation of the slag in the temperature region of 500 to 600 °C was required. Vasyutinskiy[5] followed this up with a more in-depth study of the oxidation of a similar high titania slag. This slag consisted mainly of a M_3O_5 phase, with M denoting the cations present in the phase. This phase can best represented as a $x[(Fe,Mg,Mn)O.2TiO_2].y[(Ti,Al,Cr)_2O_3.TiO_2]$ solid solution. The experimental results on the oxidation of the slag indicated three main stages. At temperatures of approximately 300 to 400 °C only slight changes in the M_3O_5 phase is observed. X-ray diffraction analysis indicated a distortion of the M_3O_5 crystal lattice. At

temperatures of up to 750 °C the formation of anatase is observed, while at higher temperatures the formation of rutile is observed. The anatase to rutile conversion temperature can range between 400 and 1000 °C, depending on the source of the anatase and the nature of the impurities in it. Decrepitation of these titania slags was explained by the oxidation of the M_3O_5 phase, resulting in the formation of anatase. As the density of anatase is less than the density of the M_3O_5 phase, this results in the rapid cracking of the slag.

Toromanoff and Habashi[6] investigated the properties of high titania slags produced at Sorel in Canada. Decrepitation of these slags during cooling was also observed. The slag consisted of a M_3O_5 phase, a glassy phase, rutile and metallic iron globules. In this Sorel slag 13.1 mass per cent of the total Ti was present as Ti^{3+}. The decrepitation process was explained by the oxidation of Ti^{3+} by Fe^{2+} during the cooling process. It was postulated that this process takes place according to the following disproportionation reaction:

$$Ti_2O_3 + FeO = 2TiO_2 + Fe^0 \ldots (R1)$$
$$\Delta G^0_{1000\,°C} = -\,71.13\ kJ.mol^{-1}$$

It was concluded that due to the difference in the coefficients of expansion of the metallic iron and the slag, the slag product cracks and decrepitates.

It is also known that ferrous and ferric pseudobrookite dissociates at certain temperatures[7]. It is possible that these disproportionation reactions can contribute to the decrepitation of the high titania slags. The disproportionation reactions are given below:

$$FeTi_2O_5 = FeTiO_3 + TiO_2 \quad [< 1150\ °C] \ldots (R2)$$
$$Fe_2TiO_5 = Fe_2O_3 + TiO_2 \quad [< 585\ °C] \ldots (R3)$$

Reid and Ward[8] found that when a solid solution of Ti_3O_5 in $FeTi_2O_5$ was formed the tendency to disproportionation decreased rapidly. It is also known that manganese and magnesium stabilize the M_3O_5 phase[9,10]. This may counter the disproportionation reactions or change the temperatures at which it occurs.

1.3 Approach to this study

Based on the available information it seems that there are several possible ways in which high titania slags can decrepitate. The following possible reasons were identified:

a) The formation of a new phase with a higher or lower molar volume.
b) A polymorphic phase change of one of the phases already present during cooling.
c) Differences in the coefficients of expansion of the metallic iron and the slag, with the metallic iron formed according to reaction R1. It is also possible that decrepitation of the slag can occur due to differences in the coefficients of expansion of other phases present in the slag.
d) Hydration of selected phases present in the slag. As no hydrated phases were previously observed in high titania slags it was however not considered as a viable option.
e) Thermal shock of the slag on cooling was considered as an option for decrepitation of the slag. However, as large blocks are cooled over extended periods of several days or weeks (depending on the size of the block) this was also considered unlikely.

To test the various possibilities, high titania slag samples produced during various smelting campaigns in a 3 MVA plasma furnace were obtained. These samples were then exposed to air under isothermal conditions in an effort to simulate the cooling process at various temperatures. Experiments were carried out between 400 and 800 °C, as this seemed to be the temperature regime where decrepitation could be expected, both from the literature information and from observations of slag blocks produced at Iscor using the 3 MVA plasma furnace.

2 EXPERIMENTAL DETAILS

Various bulk titania slag samples were produced during pilot plant campaigns carried out at Iscor using a 3 MVA plasma furnace. From these campaigns various homogeneous samples were obtained for testwork. Chemical analyses of the slag samples used in this study are shown in Table 1.

2.1 Testwork

Two types of samples were used for the testwork, these being pellets produced from milled slag and miniature slag blocks cut from larger slag lumps.

2.1.1 Experimental procedures using pellets

Slag number 7030 (see Table 1) was used to produce pellets. The slag was first milled fine (d_{50} = 121 µm). For each experiment a sample of the slag (5.00 g) was weighed, and then pelletised at 817 atmospheres in a hydraulic press to produce a cylindrical pellet. The diameter of the pellets was 15 mm, with a height of approximately 9.4 mm. Based on the dimensions of these pellets the apparent density of the pellets was calculated to be approximately 3.0 $g.cm^{-3}$. The true density of the slag is approximately 3.9 $g.cm^{-3}$. Testwork was carried out in muffle furnaces with a static air atmosphere at fixed temperatures ranging between 400 and 800 °C. Slag samples were placed in alumina crucibles, in the hot zone of the muffle furnace. At the completion of the experiment the sample was tipped from the crucible and quenched in water to enable rapid cooling of the slag. Some samples decrepitated completely to a powder when quenched, while the remainder of the samples showed little (surface decrepitation) or no visible decrepitation. The quenched samples were then dried and prepared for analyses.

2.1.2 Experimental procedures using miniature slag blocks

Slag number 7036 (see Table 1) was used to produce miniature slag blocks. These miniature blocks were cut from a large, bulk piece of slag, using a diamond coated saw. These blocks were cut in the approximate shape of a cube, with the length of each side ranging between 10 and 13 mm. Based on the mass and the measured dimensions of several of these miniature blocks, the apparent density of these blocks was calculated to be approximately 3.5 $g.cm^{-3}$. Oxidation testwork on these miniature slag blocks were carried out under the same conditions as for the pellets.

Some miniature slag blocks were also prepared (slag number 7051, Table 1) for crushing tests. These blocks were also heated in a muffle furnace at various temperatures and times as

described above before being subjected to unidirectional crushing tests using a Monsanto Tensometer. All the samples heated at 400 °C decrepitated into a powder on quenching, therefore only untreated samples and samples treated at 600 and 800 °C were used for the crushing tests.

2.2 Analytical techniques

Chemical analyses of all samples were carried out using Inductively Coupled plasma or X-ray fluorescence techniques. The oxidation states of iron and titanium in the starting slag samples were determined using wet chemical analytical techniques. X-ray diffraction and mineralogical investigations were carried out on all the samples, with polished sections prepared for standard reflected light microscopy techniques. These polished sections were also submitted for scanning electron microscopy (SEM) and electron microprobe analyses. All photographs are of back-scattered electron images, thereby providing contrasts based on atomic numbers. Rutile was used as standard for the microprobe analyses of oxygen in the various samples. This was done as the majority of the phases contained high titanium and oxygen values. This however resulted in the oxygen content of some of the standards being underestimated. For example in the case of the hematite standard, the oxygen content of the standard was underestimated by 2.7 per cent. No corrections were however made for the oxygen analyses in this paper. Selected samples were also analysed using 57-Fe Mössbauer spectroscopy.

3 RESULTS

3.1 Starting slag samples

The two main phases present in the starting slags are M_3O_5 and rutile. Details on the typical mineralogy of these slags have been given previously[11]. The chemical composition of the M_3O_5 phase in slag 7030 (see Table 1) was calculated to be $Fe_{0.30}Ti_{2.60}Al_{0.04}Mg_{0.05}Mn_{0.01}O_5$. Mössbauer spectroscopy of slag 7030, the starting material for the pelletised slag samples, was also carried out. The results indicated the presence of a single M_3O_5 phase, but with more than one type of crystallographic site for iron[12,13]. All the iron was present in the divalent oxidation state. Details of the hyperfine interaction parameters are given in Table 2. These hyperfine interaction parameters are defined by the interaction of a nucleus with its own electrons, as well as with the surrounding atoms. Grey and Ward[12] assigned the majority of the iron to strongly distorted fourfold octahedral sites in the orthorhombic pseudobrookite structure. The remainder of the iron was assigned to less distorted eightfold octahedral sites.

3.2 Results from the pelletised slag samples

Experiments on pelletised slag were carried out at temperatures between 400 and 800 °C for various times. Details of the Mössbauer results are given in Table 2. All these samples were quenched in water after the oxidation treatment. Only samples DB121 and DB125 decrepitated to powder on quenching. The remainder of the samples retained their pellet shape after quenching.

Various phases were identified in the slag samples. These included a variety of titanium and iron phases. Various minor glassy phases were also observed but these are not discussed here. The most important results are given below:

- **Sample DB109 - 800 °C for 24 hours**

The two main phases present in this sample as identified by X-ray diffraction are TiO_2 (both rutile and anatase) and M_3O_5. These two phases are intimately mixed together. Using Mössbauer spectroscopy a hematite-like phase (solid solution between hematite and ilmenite, written as M_2O_3) and a metallic iron phase were also identified. The concentration of these phases was too low to be identified by X-ray diffraction. The iron present in the M_2O_3 phase was characterised as being trivalent. A photograph of this sample is shown in Figure 1. The slag particles are shown to be finely porous, with the majority of the slag particles displaying well-defined, iron-enriched outer rims.

- **Sample DB115 - 600 °C for 24 hours**

The slag particles in this sample display a zoned texture, with iron enriched outer margins, titanium-rich mantle zones and large M_3O_5-cores with a dense and smooth appearance. Both rutile and anatase phases were identified by X-ray diffraction analyses. Iron enrichment also occurred at the edges of the cracks. Fine metallic iron precipitates were found to be present. These precipitates were associated with cracks cutting through the M_3O_5-cores. Some of the finer grained particles were completely transformed to the titanium-rich phase, but still contained iron-enriched outer rims. A typical example of this sample is shown in Figure 2.
Figure **3** shows the iron and titanium analyses from the centre of a typical particle to the rim of the particle. This illustrates the change in the composition of titanium and iron over the three phases. The chemical formula of the rim phase was calculated to be $Fe_{1.87}Ti_{0.12}Al_{0.07}Mg_{0.02}Mn_{0.01}O_3$. Mössbauer data (Table 2) indicates that the iron content of the M_2O_3 phase is trivalent. To obtain a charge balance it therefore implies that the majority of the titanium should also be trivalent. This is however unlikely, with a more probable explanation being that the titanium is tetravalent, with the iron a mixture of di- and trivalent atoms. The M/O ratio of this phase was calculated to be 0.70, which shows an oxygen deficiency in the M_2O_3 phase. This however discounts the potential correction factor that can be applied due to the underestimation of the oxygen concentration as mentioned earlier.

- **Sample DB121 - 400 °C for 24 hours**

An image of this sample is shown in Figure 4. What is immediately noticeable is the severe cracking that had taken place in this sample. Apart from the cracking the sample appears relatively dense and consists mainly of the M_3O_5 solid solution phase. The M_3O_5 phase was identified by X-ray diffraction analysis as the major phase present, with rutile being present only in trace amounts. No significant deviation in the analyses of iron and titanium could be observed across a typical crack. No Mössbauer analysis was carried out on this sample.

- **Sample DB128 – 400 °C for 48 hours**

Mössbauer analysis was carried out for a sample treated at 400 °C for 48 hours. This analysis indicated that 63 per cent of the iron atoms in the sample was present as ferrous iron, while the remainder of the iron was present in the trivalent oxidation state. The ferrous iron exhibits two components. One of the components (43 % of the iron) has parameters similar to ferropseudobrookite (M_3O_5), while the other ferrous component may be a separate ferrous phase or it may represent a second site in ferropseudobrookite that is abundantly occupied. The hyperfine interaction parameters are shown in Table 2. X-ray diffraction data and scanning electron microscopy however do not show any separate phase containing ferrous

iron. It therefore seems likely that the ferrous component is an integral part of the M_3O_5 solid solution. This is also true for the starting slag, DB100.

- **Sample DB125 - 400 °C for 384 hours**

X-ray diffraction analysis of this sample indicated only the presence of the M_3O_5 phase, with rutile and anatase either not present, or only present below the detection levels of the X-ray diffraction technique. Analyses of the M_3O_5 phase showed compositions ranging between $Fe_{0.25}Ti_{2.49}Al_{0.04}Mg_{0.05}Mn_{0.01}O_5$ and $Fe_{0.36}Ti_{2.35}Al_{0.04}Mg_{0.08}Mn_{0.04}O_5$. Mössbauer spectroscopy indicated that 45 per cent of the iron was present in the divalent oxidation state. This indicates the relatively slow rate of oxidation obtained at these low temperatures. Similar to the previous sample this sample also displays severe cracking.

3.3 Results from miniature slag blocks

Some experiments were carried out on miniature slag blocks at 400 °C to compare the results obtained with that of the pellets. These samples were also quenched in water after the oxidation treatment. It was found that only the surface of the samples decrepitated, with the bulk of the sample remaining intact. The following result are reported on:

- **DB131 - 400 °C for 24 hours**

Once again significant cracking of the sample was observed. A point in the M_3O_5 phase field with a composition of $Fe_{0.60}Ti_{2.20}Al_{0.03}Mg_{0.05}Mn_{0.03}O_5$ was analysed. Both the M_3O_5 and rutile phases were identified by X-ray diffraction analysis. Compared to sample DB121 (comparable pelletised sample) significantly more rutile was found to be present.

3.4 Results from the crushing tests on miniature slag blocks

The maximum force required for crushing of the miniature slag blocks is shown in Figure 5 as a function of the experimental conditions. Between three and four blocks were crushed for each experimental condition, with the average values obtained being shown in Figure 5. The following results were obtained:

- The untreated slag samples required significantly less force to crush than the samples treated at 600 °C for 24 hours and the samples treated at 800 °C for 24 hours.
- The samples treated at 600 °C for 24 hours required significantly more force to crush than the samples treated at 600 °C for 96 hours.
- The samples treated at 600 °C for 24 hours required significantly less force to crush than the samples treated at 800 °C for 24 hours.
- The samples treated at 600 °C for 96 hours required significantly less force to crush than the samples treated at 800 °C for 24 hours.
- No significant difference in the force required for crushing the blocks were found between the untreated slag samples and the samples treated at 600 °C for 96 hours.

The size distributions of the crushed miniature slag blocks were also evaluated in order to differentiate between the various experimental conditions used. The following statistically significant results were obtained:

- The untreated slag samples contained significantly more –500 µm material after crushing than the samples treated at 600 °C for 24 and 96 hours, as well as the samples treated at 800 °C for 24 hours.

- The samples treated at 600 °C for 24 hours were also contained significantly more –500 µm material than the samples treated at 600 °C for 96 hours and the samples treated at 800 °C for 24 hours.

No significant difference in size between the samples treated at 600 °C for 96 hours and the samples treated at 800 °C for 24 hours were found.

4 DISCUSSION

From the obtained results it appears that the samples treated at 400 °C showed the most significant propensity to decrepitate. This propensity to decrepitate seemed to decrease with an increase in temperature, with samples treated at 800 °C showing minimal signs of decrepitation. Samples treated at higher temperatures did not show the same effect as they might have sintered sufficiently to prevent decrepitation of that magnitude. At the higher temperatures the phase assemblages are also different, so that different decrepitation behaviour could possibly be expected if it occurred. The crushing tests on the miniature slag blocks also indicate that the slag treated at 800 °C requires more force to crush than the untreated slag and the slags treated at lower temperatures. This is especially so in the case of the samples treated at 400 °C which decrepitated completely on quenching.

It is assumed that the decrepitation of the samples at 400 °C is caused by the formation of the large number of cracks observed in these samples. It does not appear that these cracks are in any way associated with a new phase such as rutile. For samples DB121 and DB125 the only major phase present was the M_3O_5 phase. For sample DB131 both the M_3O_5 phase and rutile were identified to be present in significant amounts. These two phases were however not bordered by the observed cracks. The presence of rutile in the latter sample could possibly be due to the differences in the starting slag compositions of the respective samples.

It also does not appear from the available information that decrepitation of the slag occurs due to differences in the coefficients of expansion of the phases present in the slag. If this were indeed the case it would be expected that the borders between the various phases would be characterised by cracks. This was however not the case, where for example no cracks were observed at the interfaces of the M_3O_5 and rutile phases. No evidence could be found either that reaction R1 contributed in any way to the decrepitation of the slag.

The third potential mechanism for the decrepitation of the high titania slags is the possibility of a polymorphic phase change of one of the phases present in the slag. Based on the available information it seems that a polymorphic transformation of the M_3O_5 phase is the most likely cause for the decrepitation of the slag. It is for example known that Ti_3O_5 undergoes a reversible phase transformation at 190 °C[12]. In various samples produced by Haggerty and Lindsley[7] crystals in the pseudobrookite field frequently showed a tendency to form a rim with a lower reflectivity compared to the core. No variation in the iron and titanium concentration was found across the core and the rim in their study. The investigators therefore inferred that the rim represented a quenched polymorphic inversion product of pseudobrookite. As discussed previously, Vasyutinskiy[5] found that a distortion of the M_3O_5 crystal lattice occurred on oxidation of the slag samples at temperatures of approximately 400 °C. Grey and Ward[12] produced various compounds in the $Fe_xTi_{3-x}O_5$ solid solution series. X-ray powder diffraction results of these compounds show that the orthorhombic pseudobrookite cell transforms to a monoclinic cell at an approximate composition of

$Fe_{0.35}Ti_{2.65}O_5$. This distortion of the unit cell increases with increasing titanium content towards Ti_3O_5.

The chemical composition of the M_3O_5 phase in the starting slag DB100 (see Table 1) was calculated to be $Fe_{0.30}Ti_{2.60}Al_{0.04}Mg_{0.05}Mn_{0.01}O_5$. This is very close to the composition where Grey and Ward[12] found the orthorhombic-monoclinic transformation occurring. The Mössbauer results obtained in this study show that M_3O_5 solid solution phase changes as a function of time when heated at 400 °C, indicative of rather drastic changes in the crystal chemistry (see Table 2 for results). Figure 7 illustrates the differences in the Mössbauer spectra for the various slags shown in Table 2.

5 CONCLUSIONS

Decrepitation of titania slags was observed after heating at 400 °C. From the available literature and experimental information it is postulated that the decrepitation occurs due to changes in the crystal lattice of the M_3O_5 phase in the slag. The Mössbauer technique has proved extremely helpful in the investigation and it is recommended that further work be carried out using this technique to fully explain the transformations that occur. The obtained results do seem to provide some guidelines for the prevention of decrepitation of high titania slags. It seems that decrepitation can be minimised by decreasing the time the slag spends at low temperatures (approximately 400 °C). Alternatively the phase assemblages should be changed, possibly by prior oxidation, before the slag reaches these low temperatures.

6 ACKNOWLEDGEMENTS

To E.A. Viljoen and co-workers (Mintek) for carrying out electron microprobe analyses. To C.P. Visser (Iscor R&D) for carrying out the mineralogical investigations. To the Innovation Fund (Project no. 32215) of the South African Department of Arts, Culture, Science and Technology for partial funding of the project.

7 REFERENCES

1. **Okamoto A., Futamura E. and Kawamura K.** "Hydration behaviour of LD slag at autoclave test", *Trans. Iron Steel Inst. Japan, Vol. 21, No. 1, Jan. 1981, pp. 16-24*

2. **Noguchi F., Nakamura T., Ueda Y. and Yanagase T.** "Behaviour of phosphorus and sulphur in slag melts during CaO dissolution", *Australia/Japan Extractive Metallurgy Symposium, Sydney, Australia, 16-18 July 1980, Published by Australasian Institute of Mining and Metallurgy, Parkville, Victoria, 1980, pp. 479-486*

3. **Grzymek J. and Derdacka-Grzymek A.** "Physicochemical basis of sinter-disintegration complex method of aluminium oxide and cement production", *Light Metals 1990, Anaheim, California, 18-22 Feb. 1990, Published by The Minerals, Metals & Materials Society, Warrendale, Pennsylvania, 1990, pp. 149-155*

4. **Vasyutinskiy N.A. and Movsesov E.E.** "Oxidation and grinding of titanium slag", *Russian Metallurgy, 1, 1965, pp. 56-57*

5. **Vasyutinskiy N.A.** "Kinetics and mechanism of the oxidation of a titanium slag", *Russian Metallurgy, 4, 1968, pp. 29-34*

6. **Toromanoff I. and Habashi F.** "The composition of a titanium slag From Sorel", *Journal of the Less-Common Metals, 97, 1984, pp. 317-329*

7. **Haggerty S.E and Lindsley D.H.** "Stability of the pseudobrookite (Fe_2TiO_5) – ferropseudobrookite ($FeTi_2O_5$) series", *Carnegie Inst. Washington Yearbook, 68, 1970, pp. 247-249*

8. **Reid A.F and Ward J.C.** "Solid solution in the $FeTi_2O_5$-Ti_3O_5 system", *Acta Chem. Scand., 25(4), 1971, pp. 1475-1476*

9. **Grey I.E., Reid A.F. and Jones D.G.** "Reaction sequences in the reduction of ilmenite: 4 - interpretation in terms of the Fe-Ti-O and Fe-Mn-Ti-O phase diagrams", *Trans. Instn. Min. Met., 83, 1974, pp. C105-C111*

10. **Borowiec K. and Rosenqvist T.** "Phase relations and oxygen potentials in the Fe-Ti-Mg-O system", *Scandinavian Journal of Metallurgy, 14, 1985, pp. 33-43*

11. **Bessinger D., Du Plooy H., Pistorius P.C. and Visser C.** "Characteristics of some high titania slags", *Heavy Minerals 1997. Johannesburg, South African Institute of Mining and Metallurgy, 1997. Pp. 151-156*

12. **Grey I.E. and Ward J.** "An X-ray and Mössbauer study of the $FeTi_2O_5$-Ti_3O_5 system", *Journal of Solid State Chemistry, 7, 1973, pp. 300-307*

13. **Shirane G., Cox D.E. and Ruby S.L.** "Mössbauer study of isomer shift, quadrupole interaction, and hyperfine field in several oxides containing Fe^{57}", *Physical Review, 125(4), 1962, pp. 1158-1165*

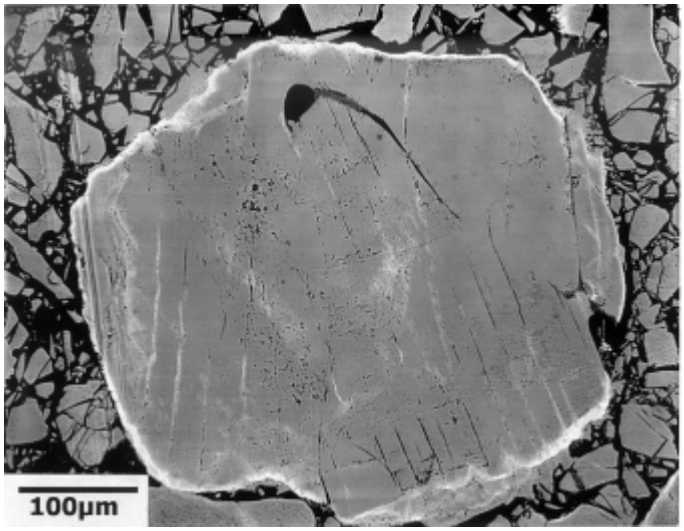

Figure 1 : Photograph of the sample treated at 800 °C for 24 hours (Sample DB109)

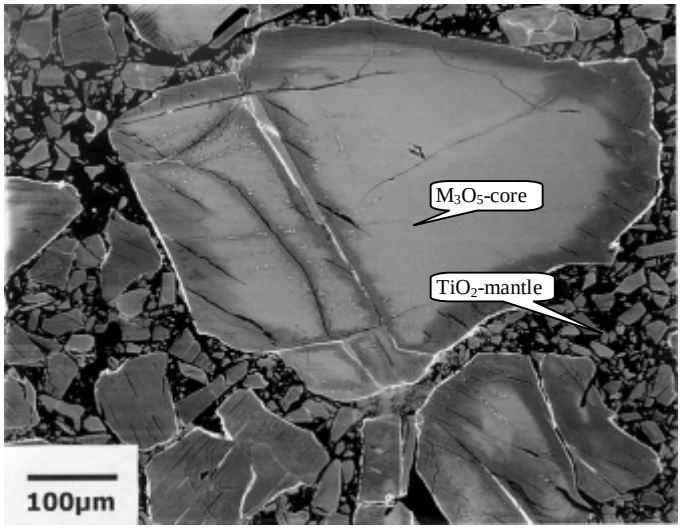

Figure 2 : Photograph of sample treated at 600 °C for 24 hours (DB115)

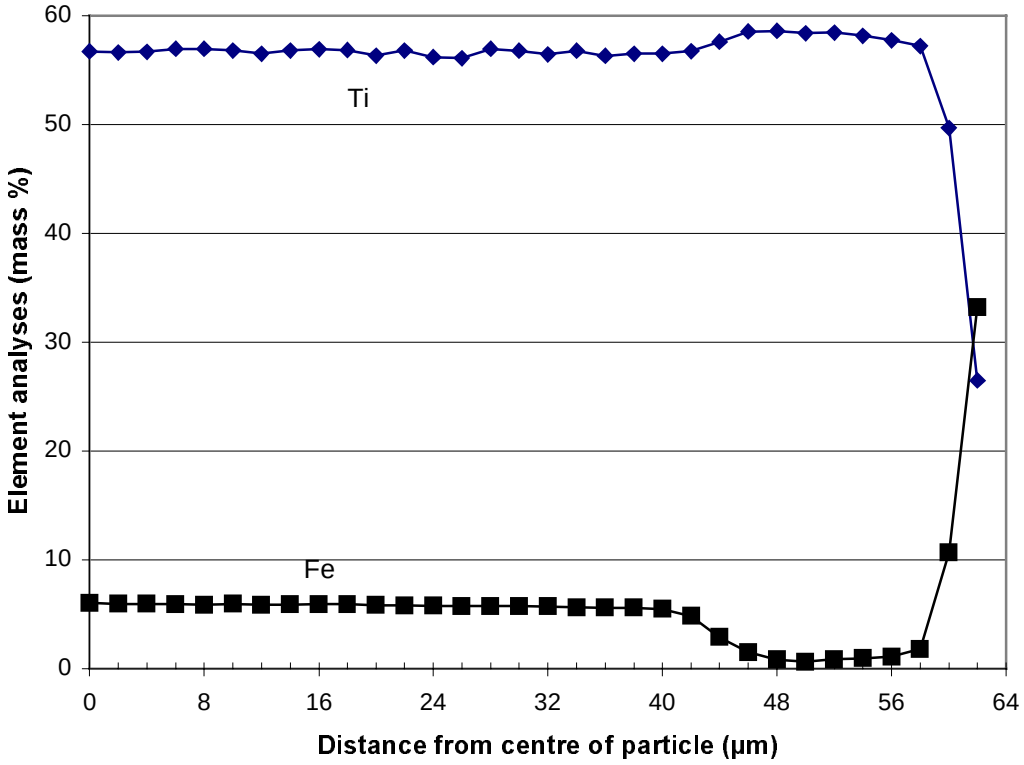

Figure 3 : Iron and titanium analyses from the centre to the rim of a typical particle treated at 600 °C for 24 hours (sample DB115)

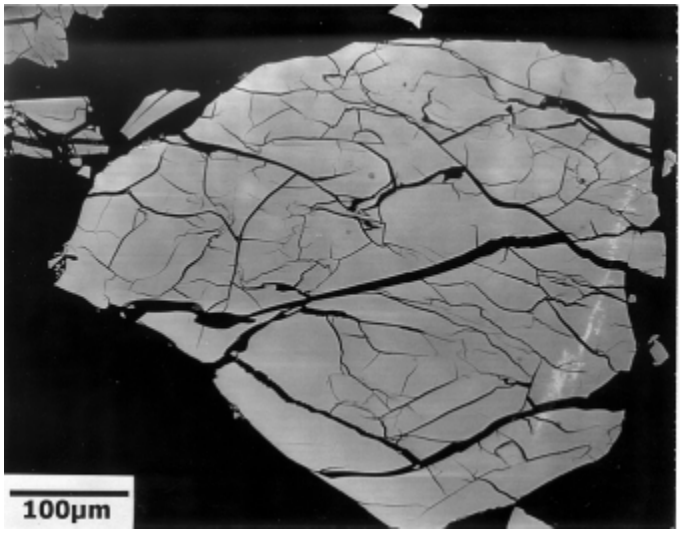

Figure 4 : Photograph of the sample treated at 400 °C for 24 hours (sample DB121)

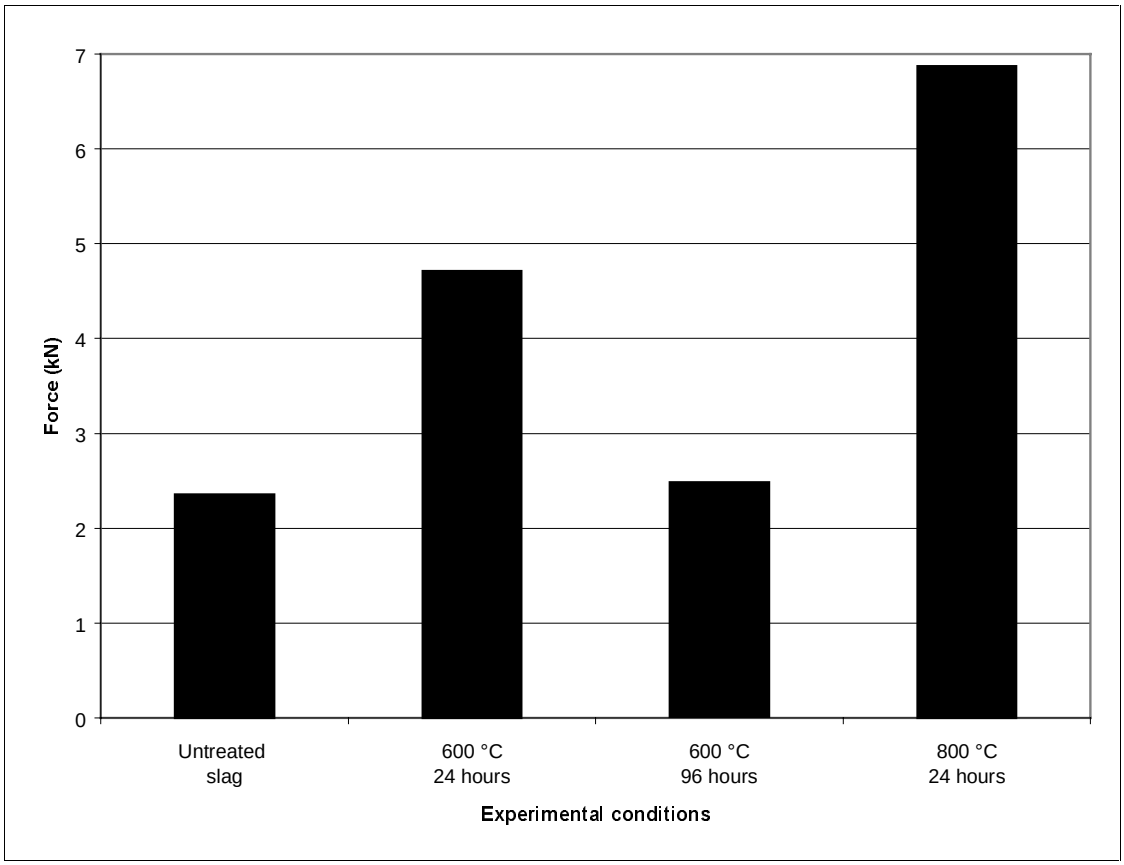

Figure 5: Maximum force applied for crushing of the miniature slag blocks

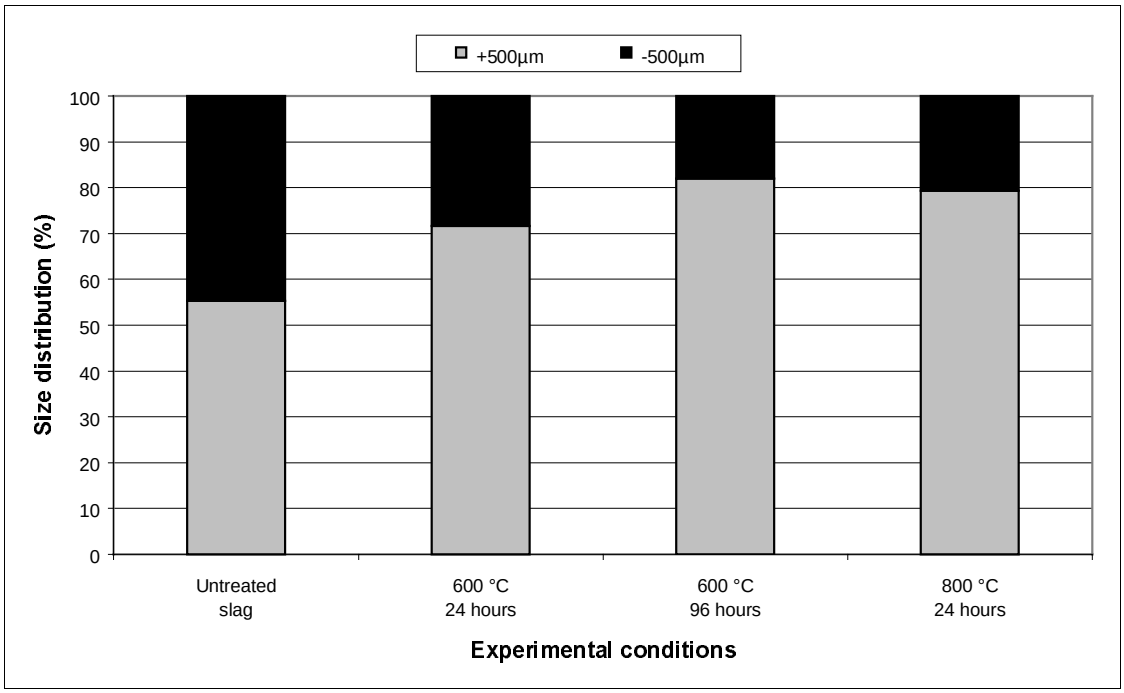

Figure 6: Size distribution of the miniature slag blocks after the crushing tests

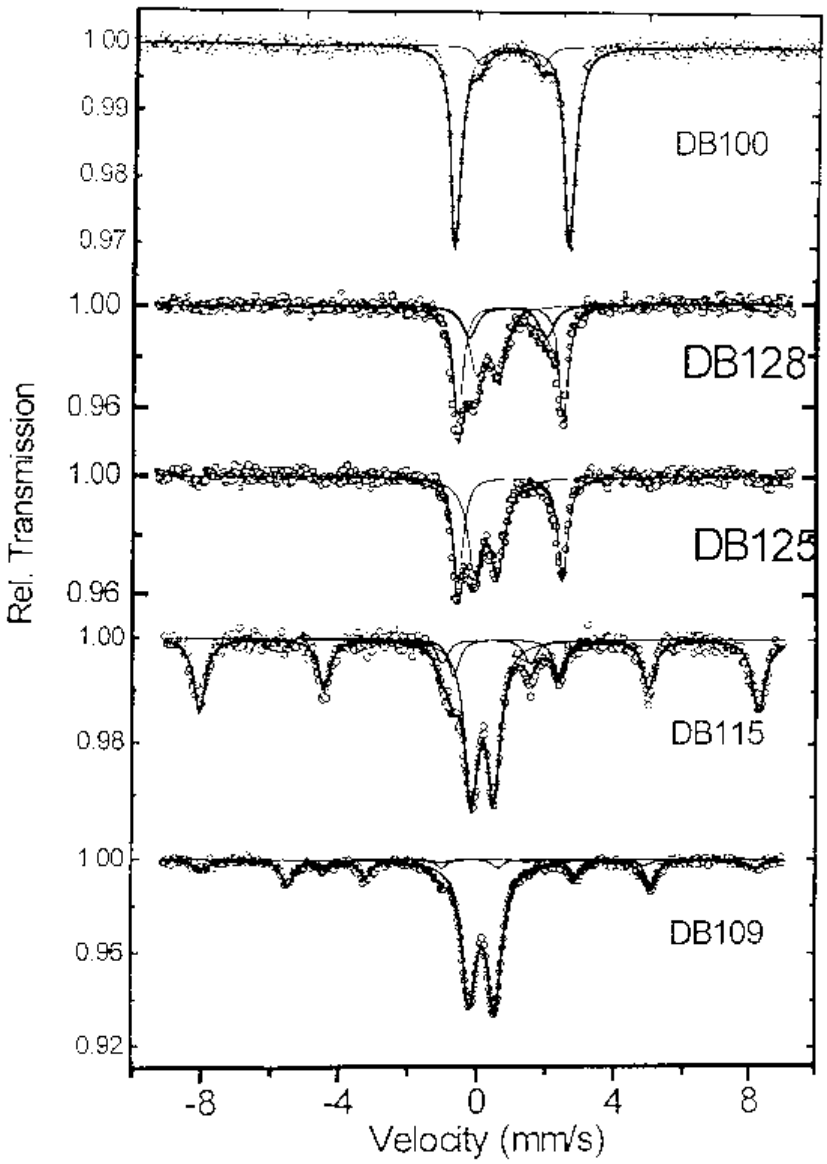

Figure 7 : Room temperature Mössbauer spectra of the various samples described in Table 2. Solid lines are theoretical fits to the data.

Table 1: Analyses of slags used as starting materials

Slag no.	Analyses no.	Analyses (mass %)												
		SiO_2	Al_2O_3	CaO	MgO	MnO	Cr_2O_3	V_2O_5	ZrO_2	Fe^0	FeO	TiO_2	Ti_2O_3	Total Ti as TiO_2
7030	DB100	1.41	1.19	0.27	1.03	1.17	0.05	0.45	0.16	< 0.1	9.8	53.9	30.4	87.7
7036	DB135	3.79	0.89	0.57	0.72	2.02	0.08	0.25	0.42	0.4	14.4	60.6	15.4	77.8
7051	DB136	1.50	0.96	0.25	1.22	1.11	0.05	0.46	0.16	0.13	8.40	52.0	33.9	89.7

Table 2: Summary of results obtained from Mössbauer spectroscopy

Sample no.	Temperature (°C)	Time (hours)	Hyperfine interaction parameters			Abundance (atom %)	Attribution
			Isomeric shift - δ ($mm.s^{-1}$)	Quadropole splitting - Δ ($mm.s^{-1}$)	B_{hf} (T)		
DB100	Starting slag		1.16 (2)	3.35 (4)	-	90 (2)	Fe^{2+} compound (ferropseudobrookite)
			1.09 (2)	1.83 (4)	-	10 (2)	
DB128	400	48	0.32 (1)	0.65 (2)	-	37 (2)	Fe^{3+} compound (pseudobrookite)
			1.09 (1)	3.07 (4)	-	43 (2)	Fe^{2+} compound (ferropseudobrookite)
			1.00 (2)	2.23 (2)	-	20 (2)	
DB125	400	384	0.39	0.68	-	55 (2)	Fe^{3+} compound (pseudobrookite)
			1.09	3.05	-	45 (2)	Fe^{2+} compound (ferropseudobrookite)
DB115	600	24	0.39 (1)	0.66 (2)	-	47 (2)	Fe^{3+} compound (pseudobrookite)
			1.07 (1)	3.07 (4)	-	11 (2)	Fe^{2+} compound (ferropseudobrookite)
			0.38 (2)	-0.20 (2)	50.8 (2)	42 (2)	Hematite-like compound
DB109	800	24	0.38 (2)	0.74 (5)	-	69 (2)	Fe^{3+} compound (pseudobrookite)
			0.02 (2)	-0.01 (3)	33.0 (1)	20 (2)	Metallic Fe
			0.36 (2)	-0.12 (5)	50.3 (2)	11 (2)	Hematite-like compound

Errors are quoted as percentage (in parenthesis)

B_{hf} – internal magnetic field